



Immune and Stroma Related Genes in Breast Cancer: A Comprehensive Analysis of Tumor Microenvironment Based on the Cancer Genome Atlas (TCGA) Database

Ming Xu[†], Yu Li[†], Wenhui Li, Qiuyang Zhao, Qiulei Zhang, Kehao Le, Ziwei Huang and Pengfei Yi*

Department of Breast and Thyroid Surgery, Union Hospital, Tongji Medical College, Huazhong University of Science and Technology, Wuhan, China

OPEN ACCESS

Edited by:

Enrico Capobianco,
University of Miami, United States

Reviewed by:

Mariane Tami Amano,
Hospital Sírio-Libanês, Brazil
Xiaoguang Li,
Johns Hopkins Medicine,
United States
Wenwen Zhang,
Nanjing Medical School, China

*Correspondence:

Pengfei Yi
yipengfei1986@126.com

[†]These authors have contributed
equally to this work

Specialty section:

This article was submitted to
Translational Medicine,
a section of the journal
Frontiers in Medicine

Received: 17 September 2019

Accepted: 12 February 2020

Published: 05 March 2020

Citation:

Xu M, Li Y, Li W, Zhao Q, Zhang Q,
Le K, Huang Z and Yi P (2020)
Immune and Stroma Related Genes in
Breast Cancer: A Comprehensive
Analysis of Tumor Microenvironment
Based on the Cancer Genome Atlas
(TCGA) Database. *Front. Med.* 7:64.
doi: 10.3389/fmed.2020.00064

Background: Tumor microenvironment is essential for breast cancer progression and metastasis. Our study sets out to examine the genes affecting stromal and immune infiltration in breast cancer progression and prognosis.

Materials and Methods: This work provides an approach for quantifying stromal and immune scores by using ESTIMATE algorithm based on gene expression matrix of breast cancer patients in TCGA database. We found differentially expressed genes (DEGs) through limma R package. Functional enrichments were accessed through Gene Ontology (GO) analysis and Kyoto Encyclopedia of Genes and Genomes (KEGG) pathway analysis. Besides, we constructed a protein-protein network, identified several hub genes in Cytoscape, and discovered functionally similar genes in GeneMANIA. Hub genes were validated with prognostic data by Kaplan-Meier analysis both in The Cancer Genome Atlas (TCGA) database and Molecular Taxonomy of Breast Cancer International Consortium (METABRIC) database and a meta-analysis of hub genes prognosis data was utilized in multiple databases. Furthermore, their relationship with infiltrating immune cells was evaluated by Tumor Immune Estimation Resource (TIMER) web tool. Cox regression was utilized for overall survival (OS) and recurrence-free survival (RFS) in TCGA database and OS in METABRIC database in order to evaluate the impact of stromal and immune scores on patients prognosis.

Results: One thousand and eighty-five breast cancer patients were investigated and 480 differentially expressed genes (DEGs) were found based on the analysis of mRNA expression profiles. Functional analysis of DEGs revealed their potential functions in immune response and extracellular interaction. Protein-protein interaction network gave evidence of 10 hub genes. Some of the hub genes could be used as predictive markers for patients prognosis. In this study, we found that tumor purity and specific immune cells infiltration varied in response to hub genes expression. The multivariate cox regression highlighted the fact that immune score played a detrimental role in overall survival (HR = 0.45, 95% CI: 0.27–0.74, $p = 0.002$) and recurrence-free survival (HR = 0.41, 95% CI: 0.22–0.77, $p = 0.006$) in TCGA database. These result was confirmed in

METABRIC database that immune score was a protector of OS (HR = 0.88, 95% CI: 0.77–0.99, $p = 0.039$).

Conclusions: Our findings promote a better understanding of the potential genes behind the regulation of tumor microenvironment and cells infiltration. Immune score should be considered as a prognostic factor for patients' survival.

Keywords: breast cancer, tumor microenvironment, immune infiltration, prognosis, ESTIMATE algorithm, The Genome Cancer Atlas database

INTRODUCTION

Over the past few years, tumor microenvironment has been one of the fastest developing and most promising fields in breast cancer research. An increasing number of studies have investigated that immune microenvironment not only modulates immunotherapy but also promotes prognosis of patients with breast cancer (1–3). To estimate the stromal and immune infiltration level of tumor and provide clues for researches on this field, Estimation of STromal and Immune cells in MAlignant Tumor tissues using Expression data (ESTIMATE) (4) is modeled and tested to calculate tumor purity, stromal and immune scores of patients via expression profile and give an overall view of tumor microenvironment. As indicated in recent work, high or intermediate immune score of breast cancer could bring better disease-free survival or overall survival (5). Other than confirming this discovery, we intended to investigate the pathways and genes that potentially affect tumor infiltration.

There are some works concerning characteristic genes that could impact tumor cellularity. Gene modifiers such as point mutations or deletions on several growth factor receptors, pattern recognition receptors, transcription factors, and apoptosis-related proteins are summarized to be associated with nonmalignant tumor microenvironment in breast cancer and affects most aspects of breast cancer biology such as tumorigenesis, progression, and metastases (6). The amount of somatic copy-number variation (SCNV) of immune genes are negatively related to immune signatures but positively related to stroma infiltration in the analysis of lung adenocarcinoma (7). Moreover, chemokines, interleukins, interferons, and their receptors are differentially expressed in different phenotypes of breast cancer with varied infiltration levels of microenvironment cells (8). On the basis of these researches, we attempted to identify pivotal genes contributed to tumor infiltration in breast cancer. Since multiple kinds of cells including tumor infiltrating lymphocytes (TILs), dendritic cells, tumor-associated macrophages (TAM), and tumor-associated neutrophils (TAN) are all related to tumor treatment and prognosis inspected in several different works (9–13), we also predicted these genes' relationships with immune cell aggregation and tumor prognosis.

MATERIALS AND METHODS

Data Collection and Preparation

The Cancer Genome Atlas-Breast Cancer (TCGA-BRCA) RNAseqV2 gene expression data and clinical data were obtained from the TCGA Data Portal (14). Altogether, 1,096

female breast cancers from TCGA with normalized gene expression and specific clinical status were collected and analyzed. Transcriptional values were Log2-transformed from the normalized fragments per kilobase transcript per million mapped reads values using R package “limma” in R 3.6.0.

We accessed Molecular Taxonomy of Breast Cancer International Consortium (METABRIC) (15) on cBioportal website (16, 17) for gene expression and clinical data. One thousand, four hundred twenty-four samples with specific genes expression and complete clinical and prognostic data were chosen and downloaded for further analysis.

ESTIMATE Algorithm and Identification of Stromal and Immune Groups

ESTIMATE algorithm (Estimation of STromal and Immune cells in MAlignant Tumor tissues using Expression data) (4) was applied to value stromal and immune microenvironment infiltration based on gene expression data. The analysis method is integrated in “estimate” R package in R 3.6.0. In ESTIMATE algorithm, the expression profiles of two independent sets of 141 genes are considered to represent the extent of tumor stromal and immune infiltrations. Thus, we extracted these expression matrixes from RNAseqV2 data to calculate stromal and immune scores in TCGA-BRCA samples. ESTIMATE score, which is the summation of stromal and immune score from individual case, is defined as tumor purity. To explore the possible association between stromal and immune score and clinical statistics, characteristics such as age at diagnosis, ER status, PR status, HER2 status, histological type, menopause status, PAM50 subtypes, pathologic T, N, M, and stage were evaluated. Unpaired *t*-test was used to compare stromal and immune scores between young (≤ 55 years old) and old patients (> 55 years old) while one-way analysis of variants and Least Significant Difference (LSD) test were used to carry out the significances of other characteristics. Since indeterminate data showed biased outcomes, we omitted them while *post hoc* was conducted.

Medians of stromal and immune scores were considered as cutoffs for high and low score group demarcation. The medians we used here were 531.15 in stromal group and 617.78 in immune group, respectively.

Identification of Valid Differentially Expressed Genes (DEGs) and Their Functional Analysis

Differentially expressed genes (DEGs), defined as dysregulated genes with $|\log_{2}FC| > 1$ and FDR < 0.05 between high and low

score groups in this study, were operated and clustered via R package “limma.”

To explore pivotal genes' function in tumor microenvironment infiltration, we intended to find genes mediated both in stromal and in immune compartment. Therefore, DEGs in stromal and immune groups were overlapped and genes were selected only when they changed synchronously in both groups (i.e., genes were upregulated or downregulated in both groups). Validated DEGs were visualized through Venn graphs and a heatmap via R package pheatmap.

Functional Enrichment, Pathway Analysis, and PPI Network of Differentially Expressed Genes (DEGs)

Using the list of DEGs above, Gene Ontology (GO) analysis and Kyoto Encyclopedia of Genes and Genomes (KEGG) pathway analysis were conducted on WebGestalt.org (18). The R package “ggplot2” was used to visualize the results of GO analysis and KEGG pathway with enrichment $p < 0.05$ and FDR < 0.1 . The top 15 pathways with highest enrichment scores were shown in biological processes (BPs) enrichment since more than 15 pathways were found during the analysis.

As we know, ESTIMATE algorithm uses 141 genes separately to calculate stromal and immune scores, in order to rule out the impact of these genes on functional network enrichment, we prudently excluded them if they are in DEGs list. After that, other valid DEGs were carried out for further protein-protein interaction (PPI) network construction. Setting minimum required interaction score as high confidence (0.7), PPI network was constructed on STRING website to elucidate potential interactions between DEGs. MCODE application (19) in Cytoscape software (20) was utilized to extract network modules and identify hub genes if they showed strong connections in the network. GeneMANIA website (21) was used to predict the relationship between hub genes and their functionally similar genes. Interaction network was downloaded and rearranged according to their interplays.

Predictive Value of Hub Genes in Survival Analysis

Hub genes were unraveled from protein-protein interactions. All samples' clinical and survival data were reanalyzed from BRCA database and the expression related prognosis were validated in METABRIC database. We divided patients into different groups by the medians of hub genes expression. Kaplan-Meier analysis was performed for survival curves and the significance was determined by log-rank, during which R packages survival and survminer in R 3.6.0 were used to analyze and sketch Kaplan-Meier curves.

Meta-analysis of Hub Genes' Survival in Organized Public Databases

We downloaded survival data with cox regression of all hub genes in PROGNOSCAN website (22), recently updated in 2019 April. In total 19 databases were included and used for meta-analysis, 18 of which are Gene Expression Omnibus (GEO)

databases and one is ArrayExpress database. The hazard ratios (HRs) of every hub gene were reorganized. Summarized HRs were illustrated using R package forest plot. Overall survival (OS) in five databases, disease free survival (DFS) in 12 databases, disease-specific survival (DSS) in three databases and disease metastasis free survival (DMFS) in nine databases were all evaluated.

Hub Genes' Correlation With Immune Cells Infiltration

To explore the relations between hub genes and the infiltrating immune cells, we utilized TIMER (Tumor IMMune Estimation Resource) web tool (23, 24) to calculate coefficients of correlation between hub genes expression and infiltrated immune cells including B cells, CD4⁺ T cells, CD8⁺ T cells, macrophages, neutrophils, and dendritic cells. The correlation heatmap was drawn using coefficients and p -values extracted from TIMER calculation via pheatmap R package.

Cox Regression and Survival Analysis

Complete clinical, pathological and prognostic data of 1,085 breast cancer patients were obtainable for further analysis. All ESTIMATE results were reorganized with clinical and pathological characteristics for subsequent statistical analysis. Quantitative stromal score and immune score were categorized into high and low groups taking medians as cutoffs. Age at diagnosis was defined as young (≤ 55 years) and old (> 55 years). Univariate and multivariate cox regression were used to shed light on the relationship between clinical patterns and the immune microenvironment in TCGA and METABRIC database. Hazard ratios and corresponding confident intervals were calculated through R package survival using survival data.

RESULTS

Stromal/Immune Scores Were Distributed Diversely in Terms of Clinical Characteristics

ESTIMATE algorithm gave stromal and immune scores for all 1,096 samples, among which 1,085 cases with clinical data were used. We firstly compared different distribution of these scores with respect to clinical characteristics as follows: age at diagnosis, ER status, PR status, HER2 status, histological type, menopause status, PAM50 subtypes, pathologic T, N, M, and tumor stage. Indeterminate data were omitted while each specific factor was inspected and analyzed as shown in **Figure 1**. Among all the characteristics displayed in **Supplementary Table S1**, we found the immune infiltration score was diversely distributed in terms of age at diagnosis, ER status, PR status, HER2 status, histological type, and PAM50 subtypes. Young patients (≤ 55 years old) showed elevated stromal scores ($p = 0.02$) but similar immune scores ($p = 0.18$) compared to old patients. Only 517 cases were defined in PAM50 subtypes. Luminal B subtype and basal-like subtype were associated with lower stromal score ($p < 0.001$) while luminal A and B subtype were less infiltrated by immune

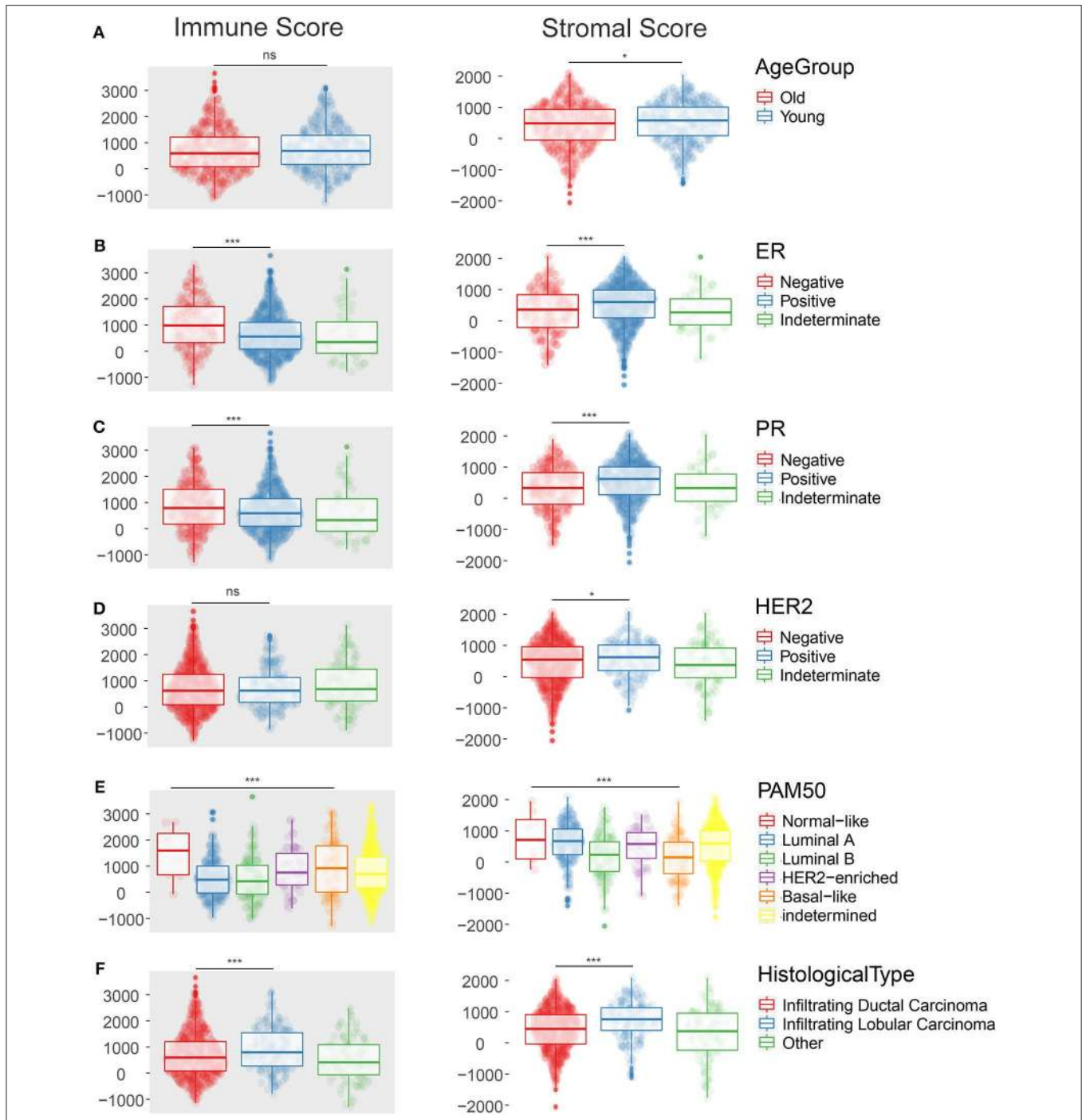


FIGURE 1 | The scatter plot shows that the immune score and the stromal score are distributed differently among clinical characteristics such as Age at diagnosis (A), ER status (B), PR status (C), HER-2 status (D), PAM50 subtypes (E), Histological type (F). * $p < 0.05$; *** $p < 0.001$; ns, not significant.

cells ($p < 0.001$). Invasive lobular carcinoma had higher level of stromal score ($p < 0.001$) but lower infiltration of immune cells ($p < 0.001$) compared with invasive ductal carcinoma, revealing the possible differences in tumor microenvironment during tumorigenesis in IDC and ILC. Positive ER and positive PR status showed same trend on lower stromal infiltration ($p < 0.001$) and higher immune infiltration ($p < 0.001$). Interestingly, positive

HER2 status was only related to lower stromal score ($p = 0.036$) but not significantly relevant to immune score ($p = 0.705$).

As for other clinical features such as menopause status, pathologic T, N, M, and tumor stage, only stromal score was significantly associated with some terms, such as pathologic T ($p = 0.003$), pathologic N ($p = 0.003$), and tumor stage ($p = 0.058$) when indeterminate data were excluded.

Up- and Down-Regulated Genes in Stromal and Immune Groups Were Overlapped to Generate Valid Differentially Expressed Genes (DEGs)

In order to evaluate the possible impact of stromal and immune scores on breast cancer, we investigated the expression patterns in different stromal and immune groups. DEGs were compared between high- and low-score stromal or immune groups with $|\log_{2}FC| < 1$ and $p < 0.05$ through R package “limma.” Total of 1,075 upregulated genes and 212 downregulated genes were found in different stromal groups. Meantime, 1,251 upregulated genes and 187 downregulated genes were identified in different immune groups.

To minimize the systematic error from group classification, the overlap of genes with same trends in both stromal and immune groups were considered as valid DEGs. Consequently, 435 overexpressed genes and 45 underexpressed genes were found (the overlap of valid DEGs was shown in Venn graph in **Figure 2A**). The heatmap of gene expression and the stromal, immune and ESTIMATE scores of 1,096 patients were shown and clustered in **Figure 2B**. The original expression data was uploaded in **Supplementary Materials**. From the clustering, we could find out that dysregulated genes showed a similar expression trend along with stromal, immune and ESTIMATE scores, indicating that they expressed coordinately and probably cooperated among certain biological processes.

Gene Ontology (GO) and Kyoto Encyclopedia of Genes and Genomes (KEGG) Analysis Showed Functional Enrichment in Immune Regulations

To explore the underlying interplay of these valid DEGs, GO analysis, and KEGG pathway enrichments were performed. As shown in **Figure 3A**, 15 biological processes (BPs) were enriched, such as immune cells activation, immune response, and cytokine metabolic processes. Ten molecular functions (MFs) including glycolysis metabolism, antigen, and immunoglobulin binding were found to be related as shown in **Figure 3B**. Seven cellular components (CCs) regarding extracellular and receptor complex, granule generation and secretion were found as shown in **Figure 3C**.

Regarding to the KEGG pathway analysis as shown in **Figure 3D**, infectious diseases related pathways were enriched such as malaria, leishmaniasis and measles. Besides, NF- κ B signaling pathway and JAK-STAT signaling pathway were also enriched, which revealed potential mechanisms and pathways activated during tumor progression. Immune processes and regulations were significantly enriched in both GO and KEGG analysis. Even though we excluded genes used for scoring, we could not deny the possibility that the enrichment result was influenced partially by scoring process. The GO identifiers/KEGG identifiers, enrichment scores and False Discovery Rates (FDRs) of the enrichment analysis was displayed below the graph.

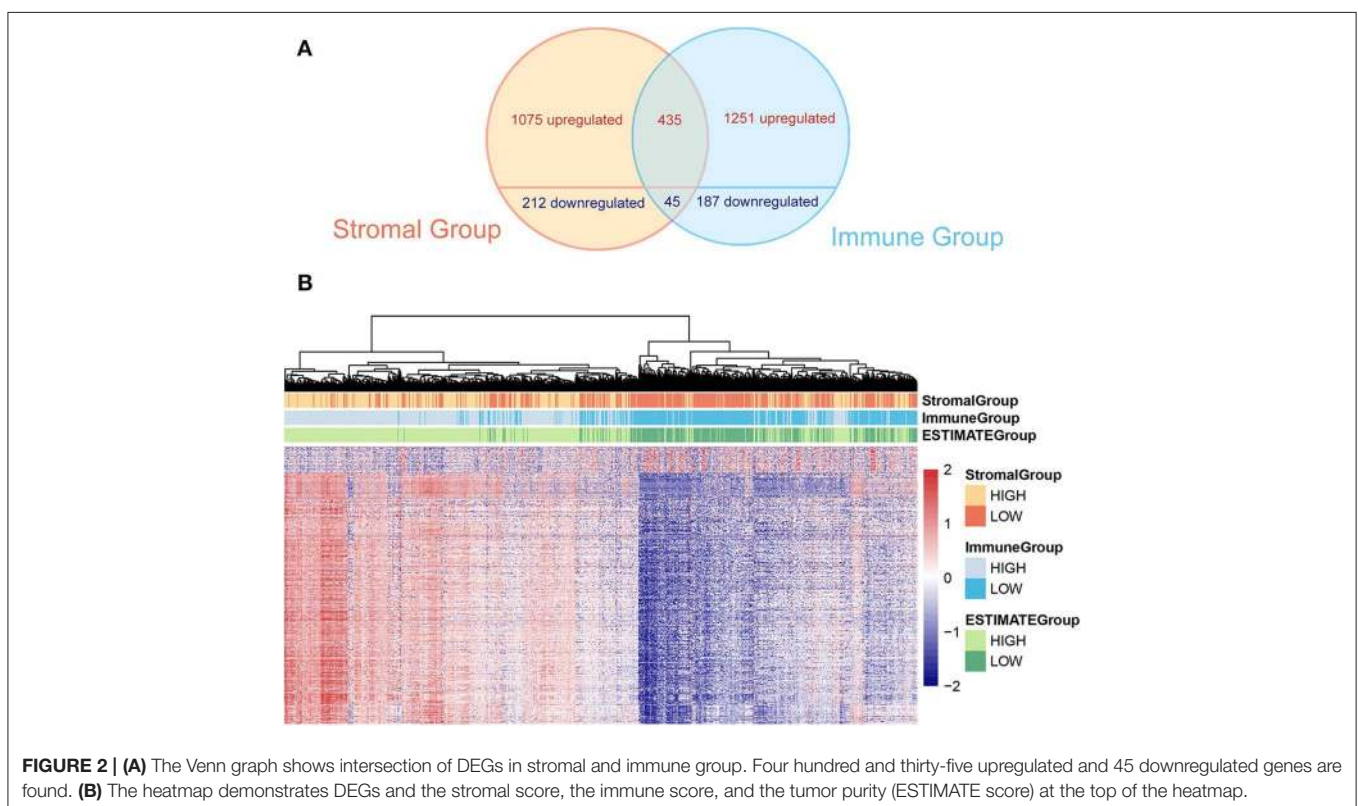


FIGURE 2 | (A) The Venn graph shows intersection of DEGs in stromal and immune group. Four hundred and thirty-five upregulated and 45 downregulated genes are found. **(B)** The heatmap demonstrates DEGs and the stromal score, the immune score, and the tumor purity (ESTIMATE score) at the top of the heatmap.

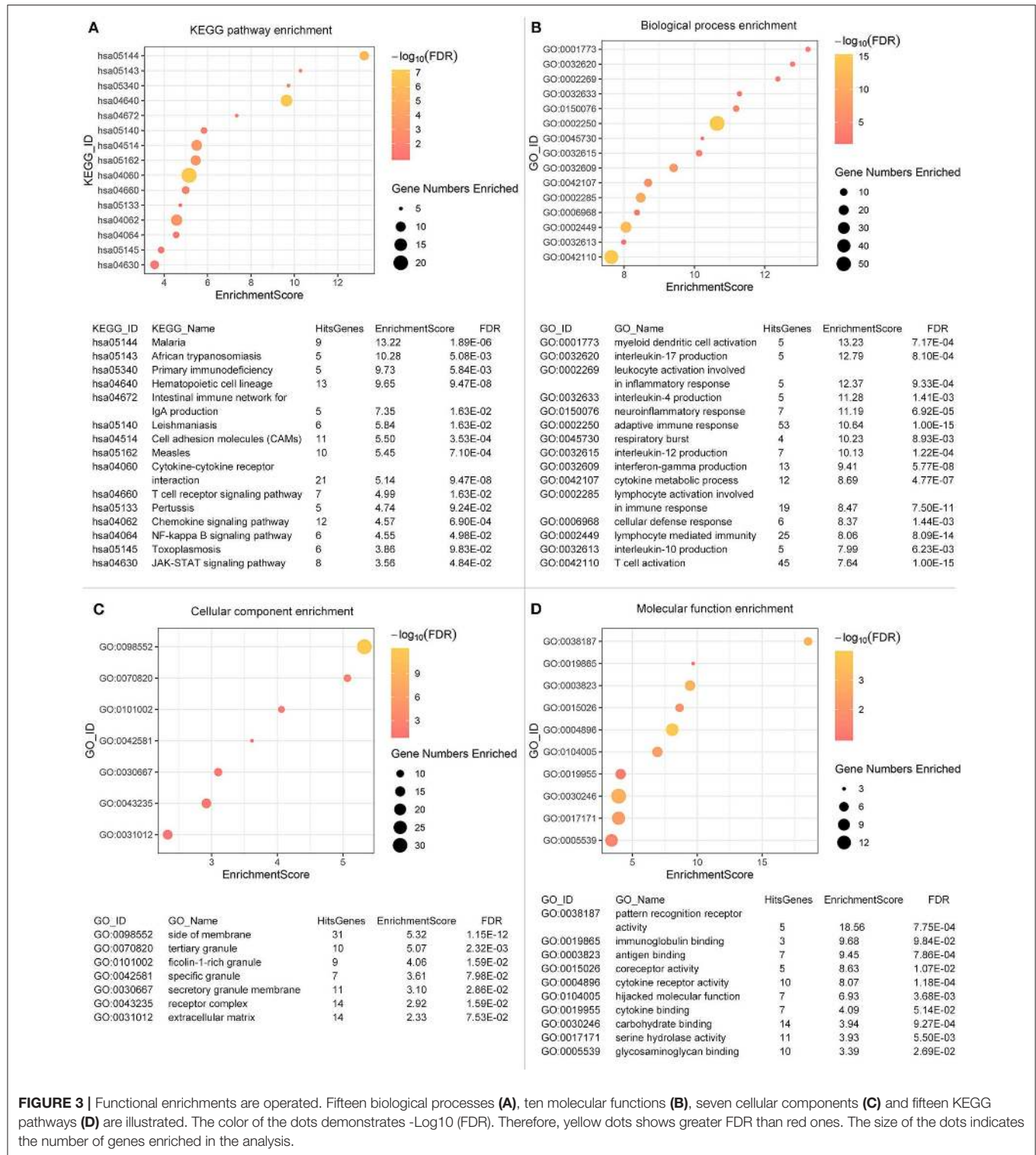
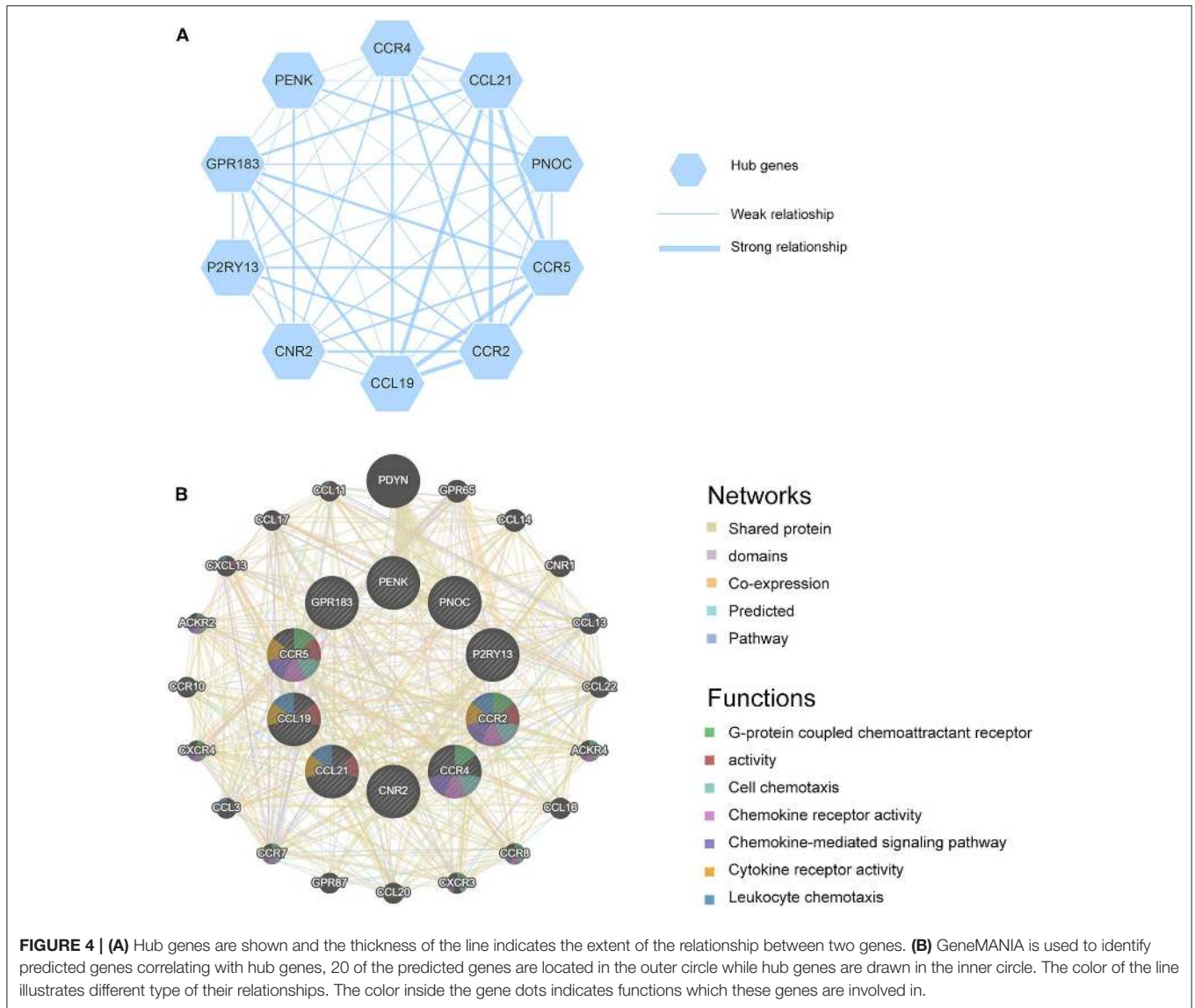


FIGURE 3 | Functional enrichments are operated. Fifteen biological processes (A), ten molecular functions (B), seven cellular components (C) and fifteen KEGG pathways (D) are illustrated. The color of the dots demonstrates $-\log_{10}(\text{FDR})$. Therefore, yellow dots shows greater FDR than red ones. The size of the dots indicates the number of genes enriched in the analysis.

Hub Genes Were Extracted From Protein-Protein Interaction (PPI) Network and Validated in Different Databases

All valid DEGs except genes employed in ESTIMATE algorithm were used to predict PPI network in STRING website. Setting

minimum required interaction score as high confidence (0.7), 191 genes were found and analyzed in STRING. All genes were mutually connected and interacted, constructing a sketch of the interplay network. Further analysis was conducted in Cytoscape and 10 genes were screened out as hub genes (CCR4,

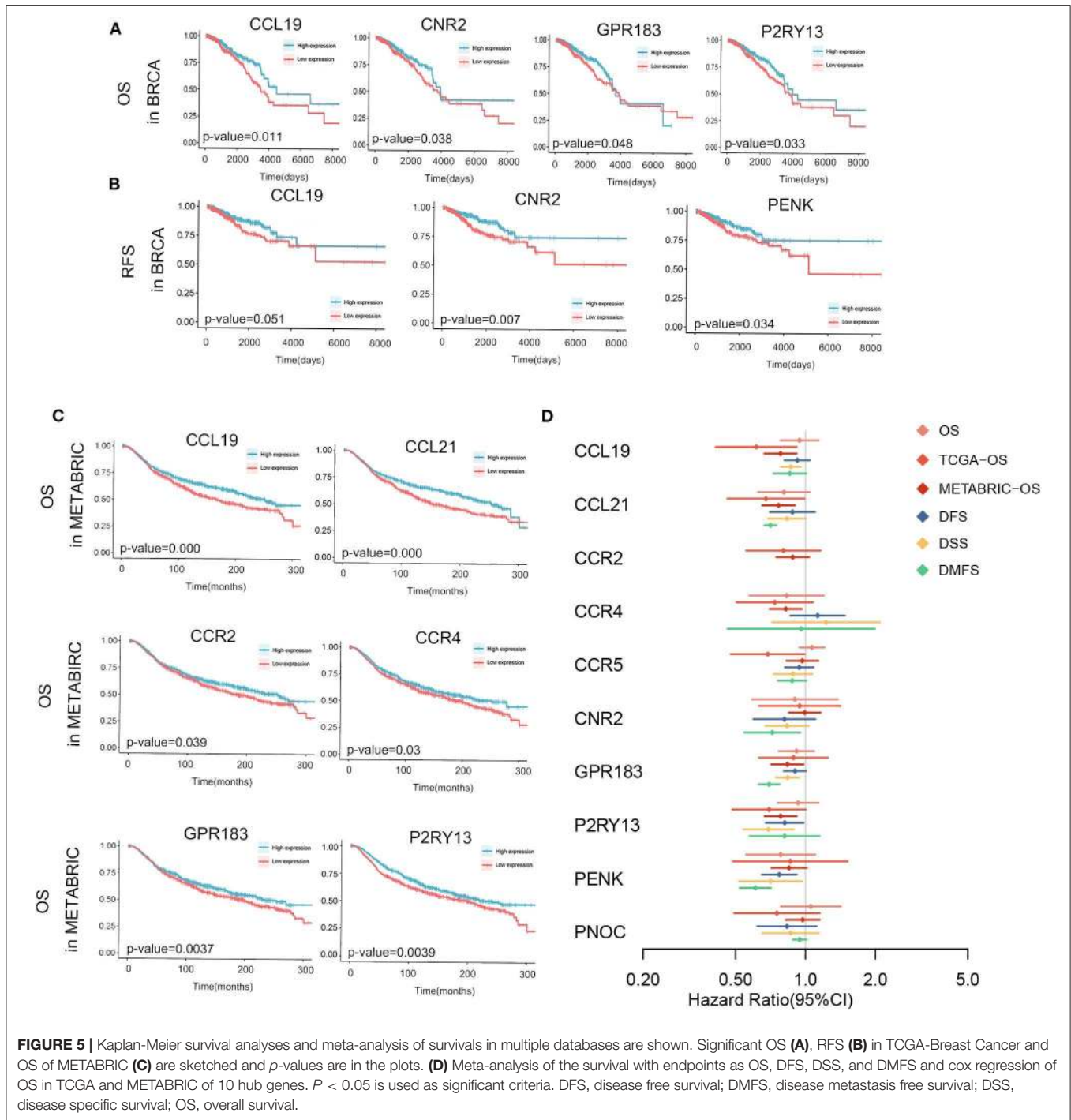


CCL21, PNOC, CCR5, CCR2, CCL19, CNR2, P2RY13, GPR183, PENK) and a potential interaction sketch map was shown in **Figure 4A**. We also uploaded hub genes to GeneMANIA website to predict functionally similar genes. As a result, twenty genes emerged as shown in **Figure 4B**, among which 17 genes had shared protein domains with hub genes, 12 genes were co-expressed with hub genes, 8 genes were co-localized with hub genes, 10 genes shared similar pathways with hub genes. We also visualized predicted functions in the network. Hub genes were arranged at the inner circle while predicted genes at the outer circle. Immune response and chemokine related functions were enriched, such as G-protein coupled chemoattractant receptor activity, cell chemotaxis, chemokine receptor activity, chemokine-mediated signaling pathway, cytokine receptor activity, leukocyte chemotaxis, and chemokine receptor binding. These results strongly supported the hypothesis that hub genes were interacted with each other

and played important roles in immune processes during the tumor progression.

Moreover, we investigated these genes in TCGA database, METABRIC database and GEO databases to find their potentials as prognostic factors. In TCGA database, higher expression of CCL19, CNR2, P2RY13 and GPR183 showed significantly higher OS rate and longer median survival time with $p < 0.05$ in **Figure 5A** and **Supplementary Figure S1**. And high expression of CCL19, CNR2, and PENK showed prolonged RFS in **Figure 5B** and **Supplementary Figure S1**. In METABRIC database, we applied Kaplan-Meier analysis of overall survivals. The relevant high expression of CCL19, CCL21, CCR2, CCR4, GPR183, or P2RY13 significantly extended patients' lifespan as shown in **Figure 5C** and **Supplementary Figure S1**.

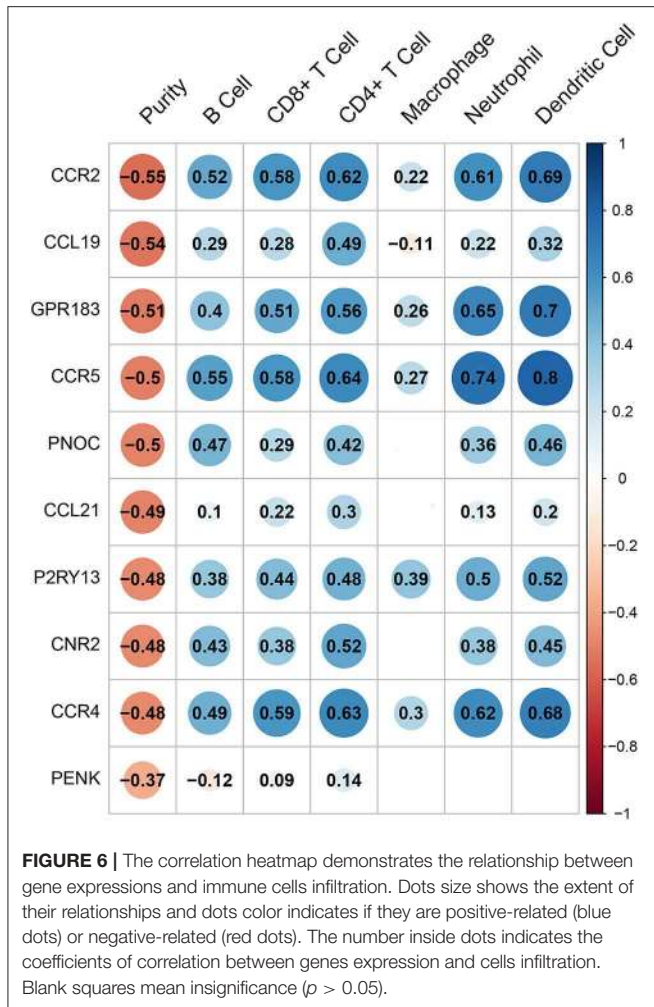
All information about 19 databases were attached in **Supplementary Table S2**. The results of meta-analysis in multiple databases of 10 hub genes and the cox regression of



genes in TCGA database and METABRIC database were together demonstrated in **Figure 5D** and **Supplementary Figure S2**. CCR2 was not in the meta-analysis since it was not evaluated in any of the multiple databases but its relationship with prognosis in TCGA and METABRIC database was demonstrated. As obviously indicated, all genes tended to be protective in patients survivals. As we can see, all genes were not significant in meta-analysis of OS. The reason of this phenomenon could be

the limited follow-up time and small sample size. Other than the results in meta-analysis, the genes which were possibly influence OS included CCL19, CCL21, CCR4, GPR183, and P2RY13. In all hub genes, P2RY13 and PENK played a significantly beneficial role in DFS as CCL19, GPR183, P2RY13, PENK in DMFS, and CCL21, CNR2, GPR183, PENK in DSS.

Overall, CCL19, CCL21, GPR183, P2RY13, and PENK were potential protective factors in breast cancer. These genes as



prognostic biomarkers in breast cancer need systematic and thorough researches in the future.

The Correlation Between Hub Genes and Immune Infiltration Was Identified

Hub genes expression was analyzed by TIMER (Tumor Immune Estimation Resource) web tool in order to predict their probable influences on immune cells infiltration including lymphoid cells such as B cells, CD4⁺ T cells, CD8⁺ T cells and myeloid cells including macrophages, neutrophils, and dendritic cells. The scatter diagrams and fitting curves generated by TIMER were attached in **Supplementary Figure S3**. Immune cells infiltration was generally linked to hub genes expression as shown in **Figure 6**. All genes were associated with tumor purity (coefficient above 0.37). Most of the genes were related to certain types of immune cells. However, we could easily tell that CCL21 and PENK have very limited correlation with immune cell infiltration while CCR2, GPR183, CCR5, and CCR4 showed a strong correlation with all immune cells except macrophages. GPR183 and CCR5 were slightly more relevant to myeloid cells infiltration while other genes showed strong mediating functions

in both lymphoid and myeloid cells. On the other aspect, macrophages were mildly affected by CCR2, GPR183, CCR5, and CCR4 while P2RY13 showed the most remarkable correlation with macrophages (coefficient = 0.39).

Cox Regression With Matrix and Immune Compartment and Clinical Characteristics

Cox regression was used to evaluate the relationship between risk factors and survival time. Univariate and multivariate cox regression were conducted using R language and forest plots were demonstrated in **Figure 7A**. In univariate analysis, young patients (≤ 55 years old) (HR = 0.60, 95% CI: 0.43–0.83, $p = 0.002$), post-menopause (HR = 2.16, 95% CI: 1.31–3.54, $p = 0.002$, compared to pre-menopause), T3&T4 (HR = 1.70, 95% CI: 1.18–2.44, $p = 0.004$, compared to T1&T2), N1&N2&M3 (HR = 2.24, 95% CI: 1.57–3.19, $p < 0.001$, compared to N0), M1 (HR = 4.41, 95% CI: 2.6–7.48, $p < 0.001$, compared to stage I & II), high immune scores (HR = 0.70, 95% CI: 0.51–0.97, $p = 0.031$) were prognostic factors. Based on the univariate analysis, we include immune score in next multivariate analysis but stromal score and ESTIMATE score were excluded since these scores were linearly dependent on each other as shown in **Supplementary Figure S4**. In multivariate analysis for overall survival, young patients (≤ 55 years old) (HR = 0.58, 95%CI: 0.35–0.95, $p = 0.032$), N0 (HR = 0.57, 95% CI: 0.37–0.88, $p = 0.012$), M0 (HR = 0.48, 95% CI: 0.25–0.84, $p = 0.011$), stage I & II (HR = 0.52, 95% CI: 0.31–0.88, $p = 0.014$), high immune scores (HR = 0.45, 95% CI: 0.27–0.74, $p = 0.002$) turned out to be protective factors.

As for recurrence-free survival (RFS), only N0 (HR = 0.45, 95% CI: 0.25–0.81, $p = 0.007$), stage I & II (HR = 0.54, 95% CI: 0.29–0.99, $p = 0.048$) and high immune score (HR = 0.41, 95% CI: 0.22–0.77, $p = 0.006$) showed their potential protective effects in multivariate cox regression (**Figure 7A**). In univariate analysis, reduced hazard ratios on recurrence-free survival could be observed in positive ER status (HR = 0.61, 95% CI: 0.39–0.94, $p = 0.026$), positive PR status (HR = 0.61, 95% CI: 0.41–0.93, $p = 0.020$), T1 (HR = 0.45, 95% CI: 0.29–0.71, $p < 0.001$) and M0 (HR = 0.25, 95% CI: 0.11–0.58, $p = 0.001$) patients group.

The univariate and multivariate cox regression of overall survival were applied in METABRIC database and immune score was confirmed to be a protector (HR = 0.88, 95% CI: 0.77–0.99, $p = 0.039$) with younger age (HR = 0.45, 95% CI: 0.35–0.57, $p = 0.039$), ER-positive (HR = 0.85, 95% CI: 0.71–1.02, $p = 0.08$), HER2-negative (HR = 0.69, 95% CI: 0.58–0.84, $p < 0.001$), smaller tumor size (HR = 0.66, 95% CI: 0.58–0.75, $p < 0.001$) and no metastasis lymph nodes (HR = 0.63, 95% CI: 0.53–0.75, $p < 0.001$) as demonstrated in **Figure 7B**. Cox regression results could be checked in **Supplementary Tables S3, S4**.

DISCUSSION

Tumor microenvironment in breast cancer has arisen concentration these years. On the basis of the fact that tumor microenvironment has manifested its influence on diagnosis, classification, treatment and prognosis, all carcinoma types are

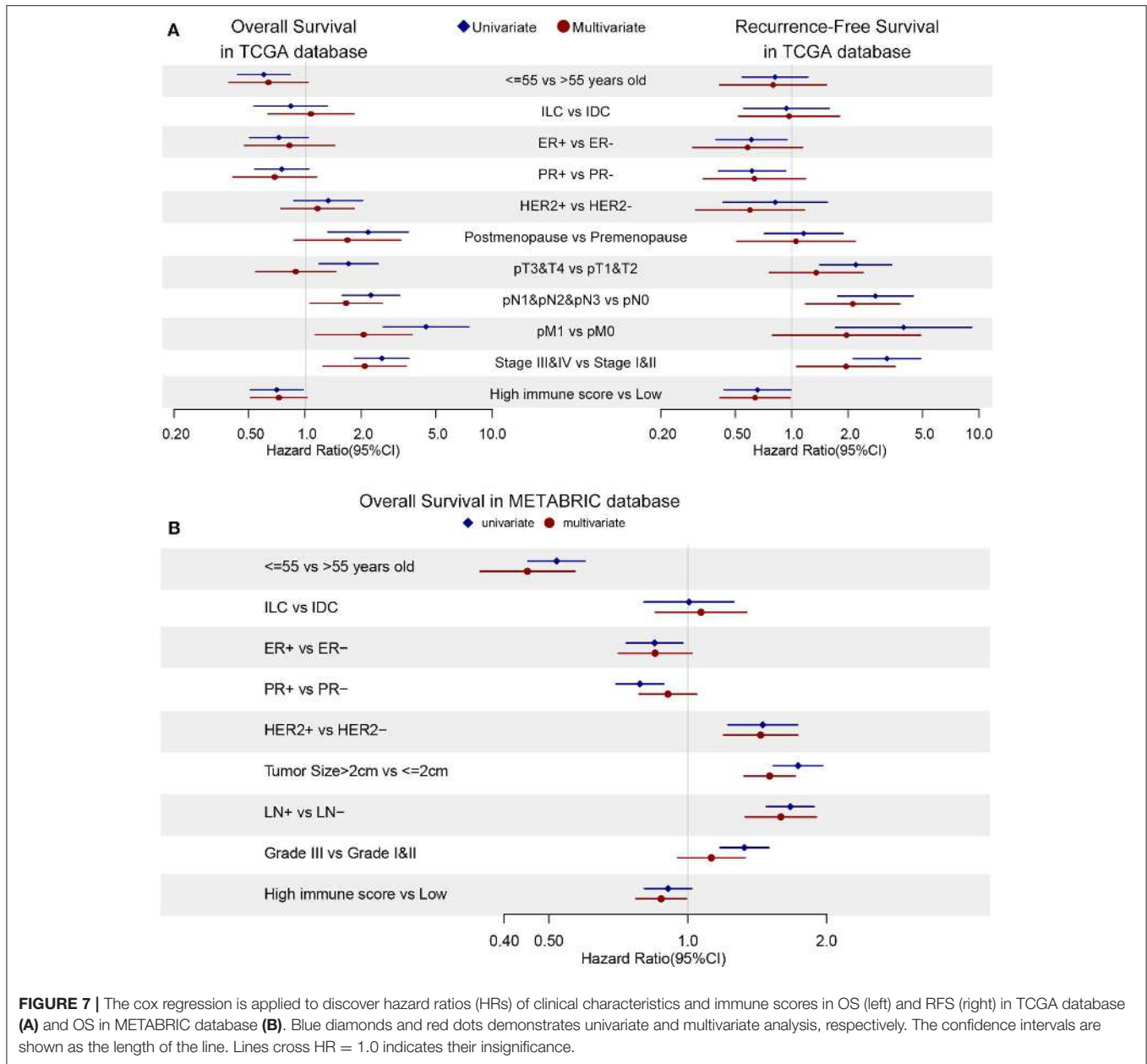


FIGURE 7 | The cox regression is applied to discover hazard ratios (HRs) of clinical characteristics and immune scores in OS (left) and RFS (right) in TCGA database **(A)** and OS in METABRIC database **(B)**. Blue diamonds and red dots demonstrates univariate and multivariate analysis, respectively. The confidence intervals are shown as the length of the line. Lines cross HR = 1.0 indicates their insignificance.

divided into different subtypes by immune genes and immune cell infiltration in several models. Pan-cancer immune analysis uses expression signatures for clustering and six immune subtypes of cancer in spite of primary sites are generated (25). The six subtypes possess distinctive characteristics on infiltrated immune cells, somatic variation, immunomodulators and prognosis. Similar analysis is applied in triple negative breast cancer that 29 immune signatures are used as criteria for clustering and defining immunity levels of high, intermediate and low (26). In a recent work, 72-gene test panel are drawn from more than 2,000 cases and tested in public and private databases for subtyping and immunity-adjusted risk of distant metastasis analysis in breast cancer (27). These findings are all focused

on clustering patients into different subtypes using immunity-related genes and cells but give little evidence on the possible mechanism of these genes or cells in tumor microenvironment.

Based on these studies, we calculated tumor purity, stromal, and immune infiltration levels based on mRNA expression. From the description of clinical characteristics and prognosis, there was a significantly positive correlation between the majority of clinical features and stromal scores but immune scores. It might suggest the independent impact of immune infiltration on prognosis and survival. The result of the cox regression was coordinated with the hypothesis. Immune score was a significant protector no matter in univariate or multivariate cox analysis. Interestingly, high immune score was found to be associated

with ER negative and PR negative status while the latter two are considered as factors for poor prognosis in breast cancer stratification and treatment. The connection between immune infiltration and ER status could be seen as well in ductal carcinoma *in situ* among women patients (28, 29). However, there is necessity that the level of immune or stromal infiltration should be detected further using flow cytometry and/or single-cell sequencing and their relationships with clinical features can be restated.

Furthermore, we bioinformatically investigated possible pathways and hub genes triggered or mediated the variation of tumor cellularity. Immune response and extracellular interactions were found during the enrichment analysis. Cell membrane activity and granule generation in CC, cytokines, membrane receptor binding and activities in MF, immune cell activation, interleukins production, immune responses in BP all combined to sketch a picture of immunity processes in tumor progression. More importantly, there are two signaling pathways highlighted in KEGG enrichment other than immunity-centered pathways, which are Janus kinase/signal transducer and activator of transcription (JAK/STAT) and NF- κ B pathway. The JAK/STAT pathway is recognized as a downstream of a variety of cytokines, hormones, and growth factors. This rapid membrane-to-nucleus signaling plays an significant role both in metabolism and in immune process (30–32). NF- κ B pathway, activated by extracellular molecules, is also a convincing induction of tumorigenesis and metastasis (33, 34). These two pathways interact with each other and modulate immune cells in tumors (35–37). Our results have given evidence of their critical roles in tumor microenvironment.

Among DEGs, 10 hub genes (CCR4, CCL21, PNO, CCR5, CCR2, CCL19, CNR2, P2RY13, GPR183, PENK) were found and their prognostic effects and relationship with infiltrated cells were predicted. The chemokines CCL19 and CCL21 were two of C-C chemokine ligands that shared the same chemokine receptor CCR7. Researchers have found that CCR7 is highly expressed on human B cells, expanded T cells instead of naïve T cells (38) and dendritic cells (39) and its expression on peripheral T cells was positively related to the chemotactic migration of T cells to CCL19 and CCL21 (40). On the other hand, CCR7 mediated chemotaxis required the existence of CCL19 or CCL21 (41). *In vitro* experiment indicated that recombinant CCL19 showed potent chemotactic activity for T-cells and B-cells but not for granulocytes and monocytes. Combined with our analysis in **Figure 6**, CCL19 showed a chemotactic role in B cells, T cells, and dendritic cells. In contrast, recombinant murine CCL21 was tested to be chemotactic for activated T cells, but not for B cells, macrophages, or neutrophils *in vitro* (42). CCL19 significantly enhanced breast cancer patients' prognosis in our work and we speculated it could work in accordance with these immune cells infiltration. In our analysis, CCL21 expression was positively correlated with T cells and dendritic cells, less correlated to B cells, neutrophils but not related to macrophages infiltration. Researchers have found that CCL21/CCR7 chemokine axis not only induced lymphangiogenesis in breast cancer (43), but also promoted breast cancer cells migration and metastasis (44). We could

further explain whether and how immune cells modulate these processes experimentally.

Chemokines receptors CCR2, CCR4, and CCR5 were extremely associated with gathering of immune cells except macrophages as in **Figure 6**. These genes are all functional receptors with several cognate chemokines and mediates chemotaxis and migration of immune cells through intracellular signaling pathways. However, these genes effect on breast cancer should be interpreted with caution since they mainly expressed in leukocytes. In Yang et al.'s work (27) on breast cancer, blood single-cell RNA-seq was used to exclude active genes in the blood and they precisely located genes that were activated in tumor tissues. More confirmation like this can be applied to chemokine receptors because the expression change of these genes can be resulted from the infiltration of leukocytes. GPR183, P2RY13 and CNR2 are all G-protein coupled receptors, in which GPR183 and P2RY13 are not only expressed in immune cells but also in breast tissues while CNR2 mostly expressed in immune organs. Their effect in immune responses and cell chemotaxis have been discovered. GPR183 mediated in immune response, intestinal immunity and inflammation (45) when activated in T cells, B cells, dendritic cells and macrophages (46–48). In glioblastoma multiforme, GPR183 contributed to chemotactic migration of THP-1 cells toward tumor (49). P2RY13, in another hand, was analyzed in lung adenocarcinoma and associated with survival of patients (50), which was similar to our analysis. But if this effect could be explained by high immune infiltration needs to be further investigated. We found P2RY13 as a promoter of high proportion of immune cells in tumor, on the contrary, P2RY13 was negatively correlated with acute inflammatory score in Crohn's disease (51). Due to different pathogenesis of Crohn's disease and breast cancer, we need to interpret the result with caution. Even though CNR2 expressed high only in the immune system, it was unraveled to enhance head and neck squamous carcinoma progression (52) and impaired prostate cancer cell migration by heterodimerized with CXCR4 (53). These genes function are not illustrated clearly, but their prognostic effect in breast cancer should be interpreted with deeper experiments.

PENK and PNO, precursor proteins of enkephalin and nociceptin, respectively, are highly expressed genes in the central neuron system as transmitters to opioid receptor and commonly work in pain transmission and perception. However, the promoter hypermethylation of PENK has been indicated in several malignancies including bladder cancer (54, 55), colorectal cancer (56) and pancreatic cells (57, 58). In researches, PENK has been reported to be required for apoptosis induction in response to activation or overexpression of p53 and p65 through NF kappa B signaling pathway (59), which is a pathway that is activated in inflammation and enriched in our functional analysis. PNO has merely been focused in cancer but it is assumed to express in immune system. Its expression could be down-regulated by LPS or IL-10 in human whole blood cultures (60). *In vivo* studies in mice and/or rats revealed the interaction between nociceptin and several inflammatory mediators in immune system such as TNF- α , IFN- γ , and IL-1 β (61–63).

To further investigate these genes relationship with immune cells, we predicted gene-immune cell interactions. It is reasonable

that higher expression of hub genes is correlated with lower tumor purity and higher immune cells infiltration. Numerous studies have attempted to summarize the suppressive functions of immune infiltration through immune cells, matrix cells (64) and immune-vascular crosstalk (65). Existing researches have recognized the critical role of mononuclear immune cells including CD4⁺ T cells, CD8⁺ T cells, macrophages, and natural killer cells (9, 66–70). In non-small cell lung cancer (NSCLC), lymphocytes especially T and B plasma cells were significantly associated with better OS (71). These results also corroborate the idea in renal cell carcinomas that different types of tumor-infiltrating immune cells modulated in different subtypes of renal carcinomas and prolonged OS or DFS (28). However, a contradictory study indicated cancer-associated fibroblasts activation correlated with tumor-associated macrophages infiltration and lymph node metastasis could promote tumor progression by mediating inflammatory reactions in triple negative breast cancers (29). Besides, stromal cells are found to act as crucial factors during chemotherapy and endocrine therapy in breast cancer (72–74). In our study, different genes had diverse correlation coefficients with different immune cells, presenting the unique function of genes in immune infiltration and tumor-immune interplay. This may suggest the immune infiltration possibly slows down tumor growth and metastases through its specific ways. But *in vitro* and *in vivo* experiments are needed to confirm their functions and interplays.

Current understanding of tumor microenvironment has showed that high immune score, indicating highly active immune cells infiltrations inside solid tumors, brings prognostic benefits including highly differentiated phenotype (75), less switch to invasive carcinoma (76), higher pathological complete response rate to neoadjuvant treatment (77) and better OS and DFS (9, 78). These results are in concordance with our analysis that immune score is a protective factor in breast cancer prognosis.

Our findings may help to understand the phenomena of stromal and immune infiltration in breast cancers. Since our analysis is totally based on bioinformatic methods, the results should be interpreted cautiously. We could only offer a relation that the hub genes and functional pathways could work in the process of tumor microenvironment and affect the prognosis of breast cancer patients, but we have very restricted evidence of their potential causal relationship. Some of our hub genes (CCL19, CCL21, CCR2, CCR4, CCR5, CNR2) are mainly expressed in immune cells or organs, resulting in the possibility that their expressions are mostly affected by immune

cells infiltration. But there is still necessity to identify their potential to predict prognosis and if possible, their function in tumor infiltration. Multi-color flow cytometry has already been used in breast cancer immunophenotyping (79) and tumor microenvironment (80). It could measure the proportion of several kinds of immune cells and sort those we are interested for *in vivo* and *in vitro* experiments. Subsequently we could clarify the specific effects of diverse immune cells to promote or prohibit tumor progression. Meanwhile, with the development of single-cell sequencing, diverse immune phenotypes in breast cancer has been illuminated (81). A combined analysis of eight patients indicated the variability of immune cells in different patients and the work also proposed the phenomenon of continuous activation in T cells in breast tumor. Abundant questions raised for further promotion on determining the interaction and crosstalk between genes and tumor-infiltrated cells in experiments.

DATA AVAILABILITY STATEMENT

The datasets generated for this study can be found in the TCGA Data Portal <https://portal.gdc.cancer.gov/> for the Cancer Genome Atlas-Breast Cancer and the cBioPortal website <https://www.cbioportal.org/> for Molecular Taxonomy of Breast Cancer International Consortium (METABRIC).

AUTHOR CONTRIBUTIONS

PY and YL proposed the topic. MX, YL, QZhuo, and QZhan contributed to the design and interpretation of the study. YL, MX, WL, KL, and ZH conducted the calculation and figures in R. All authors discussed the results and contributed to the final manuscript.

FUNDING

The research was supported by Grants 2015CKB733 and 2017CKB899 funded by Hubei Provincial Natural Science Foundation of China.

SUPPLEMENTARY MATERIAL

The Supplementary Material for this article can be found online at: <https://www.frontiersin.org/articles/10.3389/fmed.2020.00064/full#supplementary-material>

REFERENCES

1. Tekpli X, Lien T, Rossevoid AH, Nebdal D, Borgen E, Ohnstad HO, et al. An independent poor-prognosis subtype of breast cancer defined by a distinct tumor immune microenvironment. *Nat Commun.* (2019) 10:5499. doi: 10.1038/s41467-019-13329-5
2. Celebi F, Agacayak F, Ozturk A, Ilgun S, Ucuncu M, Iyigun ZE, et al. Usefulness of imaging findings in predicting tumor-infiltrating lymphocytes in patients with breast cancer. *Eur Radiol.* (2019). doi: 10.1007/s00330-019-06516-x. [Epub ahead of print].
3. Baxevanis CN, Fortis SP, Perez SA. The balance between breast cancer and the immune system: challenges for prognosis and clinical benefit from immunotherapies. *Semin Cancer Biol.* (2019). doi: 10.1016/j.semcancer.2019.12.018. [Epub ahead of print].
4. Yoshihara K, Shahmoradgoli M, Martinez E, Vegesna R, Kim H, Torres-Garcia W, et al. Inferring tumour purity and stromal and immune cell admixture from expression data. *Nat Commun.* (2013) 4:2612. doi: 10.1038/ncomms3612
5. Wang J, Li Y, Fu W, Zhang Y, Jiang J, Zhang Y, et al. Prognostic nomogram based on immune scores for breast cancer patients. *Cancer Med.* (2019) 8:5214–22. doi: 10.1002/cam4.2428

6. Flister MJ, Bergom C. Genetic modifiers of the breast tumor microenvironment. *Trends Cancer*. (2018) 4:429–44. doi: 10.1016/j.trecan.2018.04.003
7. Seo JS, Lee JW, Kim A, Shin JY, Jung YJ, Lee SB, et al. Whole exome and transcriptome analyses integrated with microenvironmental immune signatures of lung squamous cell carcinoma. *Cancer Immunol Res*. (2018) 6:848–59. doi: 10.1158/2326-6066.CIR-17-0453
8. Xiao Y, Ma D, Zhao S, Suo C, Shi J, Xue MZ, et al. Multi-omics profiling reveals distinct microenvironment characterization and suggests immune escape mechanisms of triple-negative breast cancer. *Clin Cancer Res*. (2019) 25:5002–14. doi: 10.1158/1078-0432.CCR-18-3524
9. Mahmoud SM, Paish EC, Powe DG, Macmillan RD, Grainge MJ, Lee AH, et al. Tumor-infiltrating CD8+ lymphocytes predict clinical outcome in breast cancer. *J Clin Oncol*. (2011) 29:1949–55. doi: 10.1200/JCO.2010.30.5037
10. Broz ML, Binnewies M, Boldajipour B, Nelson AE, Pollack JL, Erle DJ, et al. Dissecting the tumor myeloid compartment reveals rare activating antigen-presenting cells critical for T cell immunity. *Cancer Cell*. (2014) 26:938. doi: 10.1016/j.ccell.2014.11.010
11. Tsutsui S, Yasuda K, Suzuki K, Tahara K, Higashi H, Era S. Macrophage infiltration and its prognostic implications in breast cancer: the relationship with VEGF expression and microvessel density. *Oncol Rep*. (2005) 14:425–31. doi: 10.3892/or.14.2.425
12. Zhang Y, Cheng S, Zhang M, Zhen L, Pang D, Zhang Q, et al. High-infiltration of tumor-associated macrophages predicts unfavorable clinical outcome for node-negative breast cancer. *PLoS ONE*. (2013) 8:e76147. doi: 10.1371/journal.pone.0076147
13. Blaisdell A, Crequer A, Columbus D, Daikoku T, Mittal K, Dey SK, et al. Neutrophils oppose uterine epithelial carcinogenesis via debridement of hypoxic tumor cells. *Cancer Cell*. (2015) 28:785–99. doi: 10.1016/j.ccell.2015.11.005
14. Weinstein JN, Collisson EA, Mills GB, Shaw KR, Ozenberger BA, Ellrott K, et al. The cancer genome atlas pan-cancer analysis project. *Nat Genet*. (2013) 45:1113–20. doi: 10.1038/ng.2764
15. Curtis C, Shah SP, Chin SE, Turashvili G, Rueda OM, Dunning MJ, et al. The genomic and transcriptomic architecture of 2,000 breast tumours reveals novel subgroups. *Nature*. (2012) 486:346–52. doi: 10.1038/nature10983
16. Gao J, Aksoy BA, Dogrusoz U, Dresdner G, Gross B, Sumer SO, et al. Integrative analysis of complex cancer genomics and clinical profiles using the cBioPortal. *Sci Signal*. (2013) 6:pl1. doi: 10.1126/scisignal.2004088
17. Cerami E, Gao J, Dogrusoz U, Gross BE, Sumer SO, Aksoy BA, et al. The cBio cancer genomics portal: an open platform for exploring multidimensional cancer genomics data. *Cancer Discov*. (2012) 2:401–4. doi: 10.1158/2159-8290.CD-12-0095
18. Liao Y, Wang J, Jaehnig EJ, Shi Z, Zhang B. WebGestalt 2019: gene set analysis toolkit with revamped UIs and APIs. *Nucleic Acids Res*. (2019) 47:W199–205. doi: 10.1093/nar/gkz401
19. Bader GD, Hogue CW. An automated method for finding molecular complexes in large protein interaction networks. *BMC Bioinformatics*. (2003) 4:2. doi: 10.1186/1471-2105-4-2
20. Shannon P, Markiel A, Ozier O, Baliga NS, Wang JT, Ramage D, et al. Cytoscape: a software environment for integrated models of biomolecular interaction networks. *Genome Res*. (2003) 13:2498–504. doi: 10.1101/gr.1239303
21. Franz M, Rodriguez H, Lopes C, Zuberi K, Montojo J, Bader GD, et al. GeneMANIA update 2018. *Nucleic Acids Res*. (2018) 46:W60–4. doi: 10.1093/nar/gky311
22. Mizuno H, Kitada K, Nakai K, Sarai A. PrognScan: a new database for meta-analysis of the prognostic value of genes. *BMC Med Genomics*. (2009) 2:18. doi: 10.1186/1755-8794-2-18
23. Li T, Fan J, Wang B, Traugh N, Chen Q, Liu JS, et al. TIMER: a web server for comprehensive analysis of tumor-infiltrating immune cells. *Cancer Res*. (2017) 77:e108–10. doi: 10.1158/0008-5472.CAN-17-0307
24. Li B, Severson E, Pignon JC, Zhao H, Li T, Novak J, et al. Comprehensive analyses of tumor immunity: implications for cancer immunotherapy. *Genome Biol*. (2016) 17:174. doi: 10.1186/s13059-016-1028-7
25. Thorsson V, Gibbs DL, Brown SD, Wolf D, Bortone DS, Ou Yang TH, et al. The immune landscape of cancer. *Immunity*. (2018) 48:812–30.e14. doi: 10.1016/j.immuni.2018.03.023
26. He Y, Jiang Z, Chen C, Wang X. Classification of triple-negative breast cancers based on immunogenomic profiling. *J Exp Clin Cancer Res*. (2018) 37:327. doi: 10.1186/s13046-018-1002-1
27. Yang B, Chou J, Tao Y, Wu D, Wu X, Li X, et al. An assessment of prognostic immunity markers in breast cancer. *NPJ Breast Cancer*. (2018) 4:35. doi: 10.1038/s41523-018-0088-0
28. Zhang S, Zhang E, Long J, Hu Z, Peng J, Liu L, et al. Immune infiltration in renal cell carcinoma. *Cancer Sci*. (2019) 110:1564–72. doi: 10.1111/cas.13996
29. Zhou J, Wang XH, Zhao YX, Chen C, Xu XY, Sun Q, et al. Cancer-Associated fibroblasts correlate with tumor-associated macrophages infiltration and lymphatic metastasis in triple negative breast cancer patients. *J Cancer*. (2018) 9:4635–41. doi: 10.7150/jca.28583
30. Dodington DW, Desai HR, Woo M. JAK/STAT - emerging players in metabolism. *Trends Endocrinol Metab*. (2018) 29:55–65. doi: 10.1016/j.tem.2017.11.001
31. Villarino AV, Kanno Y, O'Shea JJ. Mechanisms and consequences of JAK-STAT signaling in the immune system. *Nat Immunol*. (2017) 18:374–84. doi: 10.1038/ni.3691
32. O'Shea JJ, Plenge R. JAK and STAT signaling molecules in immunoregulation and immune-mediated disease. *Immunity*. (2012) 36:542–50. doi: 10.1016/j.immuni.2012.03.014
33. Taniguchi K, Karin M. NF- κ B, inflammation, immunity and cancer: coming of age. *Nat Rev Immunol*. (2018) 18:309–24. doi: 10.1038/nri.2017.142
34. Pikarsky E, Porat RM, Stein I, Abramovitch R, Amit S, Kasem S, et al. NF-kappaB functions as a tumour promoter in inflammation-associated cancer. *Nature*. (2004) 431:461–6. doi: 10.1038/nature02924
35. Grivnennikov SI, Karin M. Dangerous liaisons: STAT3 and NF-kappaB collaboration and crosstalk in cancer. *Cytokine Growth Factor Rev*. (2010) 21:11–9. doi: 10.1016/j.cytogfr.2009.11.005
36. Gerondakis S, Siebenlist U. Roles of the NF-kappaB pathway in lymphocyte development and function. *Cold Spring Harb Perspect Biol*. (2010) 2:a000182. doi: 10.1101/cshperspect.a000182
37. Gerondakis S, Fulford TS, Messina NL, Grumont RJ. NF-kappaB control of T cell development. *Nat Immunol*. (2014) 15:15–25. doi: 10.1038/ni.2785
38. Hauser MA, Kindinger I, Laufer JM, Spate AK, Bucher D, Vanes SL, et al. Distinct CCR7 glycosylation pattern shapes receptor signaling and endocytosis to modulate chemotactic responses. *J Leukoc Biol*. (2016) 99:993–1007. doi: 10.1189/jlb.2VMA0915-432RR
39. Eppert BL, Motz GT, Wortham BW, Flury JL, Borchers MT. CCR7 deficiency leads to leukocyte activation and increased clearance in response to pulmonary *Pseudomonas aeruginosa* infection. *Infect Immun*. (2010) 78:2099–107. doi: 10.1128/IAI.00962-09
40. Ishizaki H, Togawa A, Tanaka-Okamoto M, Hori K, Nishimura M, Hamaguchi A, et al. Defective chemokine-directed lymphocyte migration and development in the absence of Rho guanosine diphosphate-dissociation inhibitors alpha and beta. *J Immunol*. (2006) 177:8512–21. doi: 10.4049/jimmunol.177.12.8512
41. Ponda MP, Breslow JL. Serum stimulation of CCR7 chemotaxis due to coagulation factor XIIa-dependent production of high-molecular-weight kininogen domain 5. *Proc Natl Acad Sci USA*. (2016) 113:E7059–68. doi: 10.1073/pnas.1615671113
42. Hedrick JA, Zlotnik A. Identification and characterization of a novel beta chemokine containing six conserved cysteines. *J Immunol*. (1997) 159:1589–93.
43. Tutunea-Fatan E, Majumder M, Xin X, Lala PK. The role of CCL21/CCR7 chemokine axis in breast cancer-induced lymphangiogenesis. *Mol Cancer*. (2015) 14:35. doi: 10.1186/s12943-015-0306-4
44. Muller A, Homey B, Soto H, Ge N, Catron D, Buchanan ME, et al. Involvement of chemokine receptors in breast cancer metastasis. *Nature*. (2001) 410:50–6. doi: 10.1038/35065016
45. Willinger T. Oxysterols in intestinal immunity and inflammation. *J Intern Med*. (2019) 285:367–80. doi: 10.1111/joim.12855
46. Barington L, Wanke F, Niss Arfelt K, Holst PJ, Kurschus FC, Rosenkilde MM. EB12 in splenic and local immune responses and in autoimmunity. *J Leukoc Biol*. (2018) 104:313–22. doi: 10.1002/JLB.2VMR1217-510R
47. Preuss I, Ludwig MG, Baumgarten B, Bassilana F, Gessier F, Seuwen K, et al. Transcriptional regulation and functional characterization of the

- oxysterol/EBI2 system in primary human macrophages. *Biochem Biophys Res Commun.* (2014) 446:663–8. doi: 10.1016/j.bbrc.2014.01.069
48. Gatto D, Wood K, Caminschi I, Murphy-Durland D, Schofield P, Christ D, et al. The chemotactic receptor EBI2 regulates the homeostasis, localization and immunological function of splenic dendritic cells. *Nat Immunol.* (2013) 14:446–53. doi: 10.1038/ni.2555
 49. Eibinger G, Fauler G, Bernhart E, Frank S, Hammer A, Wintersperger A, et al. On the role of 25-hydroxycholesterol synthesis by glioblastoma cell lines. Implications for chemotactic monocyte recruitment. *Exp Cell Res.* (2013) 319:1828–38. doi: 10.1016/j.yexcr.2013.03.025
 50. Li L, Peng M, Xue W, Fan Z, Wang T, Lian J, et al. Integrated analysis of dysregulated long non-coding RNAs/microRNAs/mRNAs in metastasis of lung adenocarcinoma. *J Transl Med.* (2018) 16:372. doi: 10.1186/s12967-018-1732-z
 51. Rybaczuk L, Rozmiarek A, Circle K, Grants I, Needleman B, Wunderlich JE, et al. New bioinformatics approach to analyze gene expressions and signaling pathways reveals unique purine gene dysregulation profiles that distinguish between CD and UC. *Inflamm Bowel Dis.* (2009) 15:971–84. doi: 10.1002/ibd.20893
 52. Liu C, Sadat SH, Ebisumoto K, Sakai A, Panuganti BA, Ren S, et al. Cannabinoids promote progression of HPV positive head and neck squamous cell carcinoma via p38 MAPK activation. *Clinical Cancer Res.* (2020) doi: 10.1158/1078-0432.CCR-18-3301
 53. Scarlett KA, White EZ, Coke CJ, Carter JR, Bryant LK, Hinton CV. Agonist-induced CXCR4 and CB2 heterodimerization inhibits Galpha13/RhoA-mediated migration. *Molecular Cancer Res.* (2018) 16:728–39. doi: 10.1158/1541-7786.MCR-16-0481
 54. Chung W, Bondaruk J, Jelinek J, Lotan Y, Liang S, Czerniak B, et al. Detection of bladder cancer using novel DNA methylation biomarkers in urine sediments. *Cancer Epidemiol Biomarkers Prev.* (2011) 20:1483–91. doi: 10.1158/1055-9965.EPI-11-0067
 55. Zhang Y, Fang L, Zang Y, Xu Z. Identification of core genes and key pathways via integrated analysis of gene expression and DNA methylation profiles in bladder cancer. *Med Sci Monit.* (2018) 24:3024–33. doi: 10.12659/MSM.909514
 56. Roperch JP, Incitti R, Forbin S, Bard F, Mansour H, Mesli F, et al. Aberrant methylation of NPY, PENK, and WIF1 as a promising marker for blood-based diagnosis of colorectal cancer. *BMC Cancer.* (2013) 13:566. doi: 10.1186/1471-2407-13-566
 57. Jin T, Hao J, Fan D. Nicotine induces aberrant hypermethylation of tumor suppressor genes in pancreatic epithelial ductal cells. *Biochem Biophys Res Commun.* (2018) 499:934–40. doi: 10.1016/j.bbrc.2018.04.022
 58. Azizi M, Fard-Esfahani P, Mahmoodzadeh H, Fazeli MS, Azadmanesh K, Zeinali S, et al. MiR-377 reverses cancerous phenotypes of pancreatic cells via suppressing DNMT1 and demethylating tumor suppressor genes. *Epigenomics.* (2017) 9:1059–75. doi: 10.2217/epi-2016-0175
 59. McTavish N, Copeland LA, Saville MK, Perkins ND, Spruce BA. Proenkephalin assists stress-activated apoptosis through transcriptional repression of NF-kappaB- and p53-regulated gene targets. *Cell Death Differ.* (2007) 14:1700–10. doi: 10.1038/sj.cdd.4402172
 60. Zhang L, Stuber F, Stamer UM. Inflammatory mediators influence the expression of nociceptin and its receptor in human whole blood cultures. *PloS ONE.* (2013) 8:e74138. doi: 10.1371/journal.pone.0074138
 61. Goldfarb Y, Reinscheid RK, Kuskov AW. Orphanin FQ/nociceptin interactions with the immune system in vivo: gene expression changes in lymphoid organs and regulation of the cytokine response to staphylococcal enterotoxin A. *J Neuroimmunol.* (2006) 176:76–85. doi: 10.1016/j.jneuroim.2006.04.008
 62. Buzas B, Rosenberger J, Kim KW, Cox BM. Inflammatory mediators increase the expression of nociceptin/orphanin FQ in rat astrocytes in culture. *GLIA.* (2002) 39:237–46. doi: 10.1002/glia.10106
 63. Gavioli EC, de Medeiros IU, Monteiro MC, Calo G, Romao PR. Nociceptin/orphanin FQ-NOP receptor system in inflammatory and immune-mediated diseases. *Vitam Horm.* (2015) 97:241–66. doi: 10.1016/bs.vh.2014.11.003
 64. Binnewies M, Roberts EW, Kersten K, Chan V, Fearon DF, Merad M, et al. Understanding the tumor immune microenvironment (TIME) for effective therapy. *Nat Med.* (2018) 24:541–50. doi: 10.1038/s41591-018-0014-x
 65. Huang Y, Kim BYS, Chan CK, Hahn SM, Weissman IL, Jiang W. Improving immune-vascular crosstalk for cancer immunotherapy. *Nat Rev Immunol.* (2018) 18:195–203. doi: 10.1038/nri.2017.145
 66. Ali HR, Provenzano E, Dawson SJ, Blows FM, Liu B, Shah M, et al. Association between CD8+ T-cell infiltration and breast cancer survival in 12,439 patients. *Ann Oncol.* (2014) 25:1536–43. doi: 10.1093/annonc/mdu191
 67. Bates GJ, Fox SB, Han C, Leek RD, Garcia JE, Harris AL, et al. Quantification of regulatory T cells enables the identification of high-risk breast cancer patients and those at risk of late relapse. *J Clin Oncol.* (2006) 24:5373–80. doi: 10.1200/JCO.2006.05.9584
 68. Rath M, Muller I, Kropf P, Closs EI, Munder M. Metabolism via arginase or nitric oxide synthase: two competing arginine pathways in macrophages. *Front Immunol.* (2014) 5:532. doi: 10.3389/fimmu.2014.00532
 69. Vivier E, Tomasello E, Baratin M, Walzer T, Ugolini S. Functions of natural killer cells. *Nat Immunol.* (2008) 9:503–10. doi: 10.1038/ni1582
 70. Qiu SQ, Waaijer SJH, Zwager MC, de Vries EGE, van der Veegt B, Schroder CP. Tumor-associated macrophages in breast cancer: innocent bystander or important player? *Cancer Treat Rev.* (2018) 70:178–89. doi: 10.1016/j.ctrv.2018.08.010
 71. Edlund K, Madjar K, Mattsson JSM, Djureinovic D, Lindskog C, Brunnstrom H, et al. Prognostic impact of tumor cell programmed death ligand 1 expression and immune cell infiltration in NSCLC. *J Thorac Oncol.* (2019) 14:628–40. doi: 10.1016/j.jtho.2018.12.022
 72. Majidinia M, Yousefi B. Breast tumor stroma: a driving force in the development of resistance to therapies. *Chem Biol Drug Des.* (2017) 89:309–18. doi: 10.1111/cbdd.12893
 73. McMillin DW, Negri JM, Mitsiades CS. The role of tumour-stromal interactions in modifying drug response: challenges and opportunities. *Nat Rev Drug Discov.* (2013) 12:217–28. doi: 10.1038/nrd3870
 74. Marra A, Viale G, Curigliano G. Recent advances in triple negative breast cancer: the immunotherapy era. *BMC Med.* (2019) 17:90. doi: 10.1186/s12916-019-1326-5
 75. Dennison JW, Shahmoradgoli M, Liu W, Ju Z, Meric-Bernstam F, Perou CM, et al. High intratumoral stromal content defines reactive breast cancer as a low-risk breast cancer subtype. *Clinical Cancer Res.* (2016) 22:5068–78. doi: 10.1158/1078-0432.CCR-16-0171
 76. Gil Del Alcazar CR, Huh SJ, Ekram MB, Trinh A, Liu LL, Beca F, et al. Immune escape in breast cancer during in situ to invasive carcinoma transition. *Cancer Discov.* (2017) 7:1098–115. doi: 10.1158/2159-8290.CD-17-0222
 77. West NR, Milne K, Truong PT, Macpherson N, Nelson BH, Watson PH. Tumor-infiltrating lymphocytes predict response to anthracycline-based chemotherapy in estrogen receptor-negative breast cancer. *Breast Cancer Res.* (2011) 13:R126. doi: 10.1186/bcr3072
 78. Dieci MV, Tsvetkova V, Orvieto E, Piacentini F, Ficarra G, Griguolo G, et al. Immune characterization of breast cancer metastases: prognostic implications. *Breast Cancer Res.* (2018) 20:62. doi: 10.1186/s13058-018-1003-1
 79. Trintinaglia L, Bandinelli LP, Grassi-Oliveira R, Petersen LE, Anzolin M, Correa BL, et al. Features of immunosenescence in women newly diagnosed with breast cancer. *Front Immunol.* (2018) 9:1651. doi: 10.3389/fimmu.2018.01651
 80. Young YK, Bolt AM, Ahn R, Mann KK. Analyzing the tumor microenvironment by flow cytometry. *Methods Mol Biol.* (2016) 1458:95–110. doi: 10.1007/978-1-4939-3801-8_8
 81. Azizi E, Carr AJ, Plitas G, Cornish AE, Konopacki C, Prabhakaran S, et al. Single-cell map of diverse immune phenotypes in the breast tumor microenvironment. *Cell.* (2018) 174:1293–308.e36. doi: 10.1016/j.cell.2018.05.060

Conflict of Interest: The authors declare that the research was conducted in the absence of any commercial or financial relationships that could be construed as a potential conflict of interest.

Copyright © 2020 Xu, Li, Li, Zhao, Zhang, Le, Huang and Yi. This is an open-access article distributed under the terms of the Creative Commons Attribution License (CC BY). The use, distribution or reproduction in other forums is permitted, provided the original author(s) and the copyright owner(s) are credited and that the original publication in this journal is cited, in accordance with accepted academic practice. No use, distribution or reproduction is permitted which does not comply with these terms.